Available online at https://sej.journals.ekb.eg/

FACULTY OF ENGINEERING – SOHAG UNIVERSITY

Sohag Engineering Journal (SEJ), VOL. 2, NO. 2, SEPTEMBER 2022

Numerical Parametric Study of RC Beams Strengthened with Fabric-Reinforced Cementitious Matrix (FRCM)

Mohamed Nagah[a*], Ahmed Arafa[b], Yehia. A. Hassanean[c], and Ahmed Attia M. Drar[d]

[a]*Demonstrator, Civil Department, Faculty of Engineering, Sohag University, Egypt,*

E-mail: mohamed.nagah2019@eng.sohag.edu.eg

[b]*Lecturer, Civil Department, Faculty of Engineering, Sohag University, Egypt,*

E-mail: ahmed_arafa@eng.sohag.edu.eg

[c]*Professor, Civil Department, Faculty of Engineering, Assiut University, Egypt,*

E-mail: yehia1@eng.aun.edu.eg

[d]*Assistant professor, Civil Department, Faculty of Engineering, Sohag University, Egypt, E-mail: attya85@yahoo.com & ahmed.atya@eng.sohag.edu.eg*

Abstract

The epoxy bonded system has several drawbacks like low resistance fire. Fabric-reinforced cementitious matrix (FRCM) which comprises of fabric textiles buried in an inorganic mortar resulting in a competitive technology on strengthening RC structures. The numerical studies of this technique are slightly limited. This study presented a finite element modeling of the flexure behavior of RC beams reinforced with FRCM layers. This modeling is verified using a previous experimental study which indicates a good verification between numerical and experimental results. Large-scale beams were proposed. The number and type of FRCM layers with five different reinforcement ratios are investigated as studied parameters in this study. Moreover, two shapes of FRCM layers were used. The results revealed that both ultimate and total workability of the examined beams improve by increasing both reinforcement ratio and number of FRCM layers. U-wrapped layer had a significant improvement for beams behavior compared with the straight layer.

 DOI: 10.21608/SEJ.2022.154757.1017

Keywords: FRP, FRCM, FEM, Strengthening, RC beams.

1. INTRODUCTION

External fiber-reinforced polymer (FRP) materials have been discussed in many past studies [1-4]. Where, the FRP has many advantages like high tensile capacity, modulus of elasticity, high strength compared to weight ratio, and resisting corrosion. The FRP composites comprise two main elements fibers and adhesive material called epoxy. Although, there are several advantages to using epoxy, like its ability to work as an effective adhesive material to link fabrics and concrete and its ability to transmit load to the fabric. However, the bonded FRP strengthening still presents several drawbacks. Where it's debonding when exposed to the fire [5-6] and high temperature [7-9]. Moreover, it has lack of resistance to UR, low permeability, and diffusion tightness. These drawbacks lead to strength shortage and have an impact on the external FRP bond's capacity of the inadequate beams. To treat these drawbacks, the FRCM has been lately presented. In fabric-reinforced cementitious matrix (FRCM), a structural reinforcing mesh, many types of fabric or textile with open structure as shown in Fig. 1, is used instead of fiber sheets embedded in an inorganic mortar called cement mortars.

* Corresponding author: mohamed.nagah2019@eng.sohag.edu.eg

(a) (b) (c)

Fig.1 Fiber meshes Types: (**a**) PBO; (**b**) carbon; (**c**) glass.

The strengthening of RC beams with FRCM was studied in several experimental research. However, few theoretical studies discussed this matter. Luciano Ombres, [10] conducted an experimental and theoretical investigation on RC beams reinforced with a high-strength composite material based on mortar. The longitudinal reinforcement ratio and the layers number were discussed by Ombres, [10]. Where, both yielding and ultimate capacity increased by utilizing PBO-FRCM and it typically enhancement the flexural capacity of the inadequate beams. Also, the ductility reduces by increasing both reinforcement ratio and the number of layers. Moreover, the failure mode depended on the number of layers. The influence of the FRCM type and its axial stiffness on flexural capacity was discussed by Abdulla Jabr, et al, [11]. They investigated the effect of the main steel ratio and the fabric type (PBO, glass, and carbon fibers) on the studied beams. Utilizing PBO – FRCM accomplished a great effect on raising the ultimate capacity of examined beams. On the contrary, a little increment within the ultimate capacity of the inspected beams was recorded when using the other two types. Moreover, the increasing in extreme load depended on the axial stiffness ratios (EA_{FRCM}/EA_{steel}). Furthermore, Mohammed Elghazy, et al, [12] presented an experimental study to evaluate the flexural capacity of RC beams reinforced with FRCM layers under several parameters' studies like corrosion ratio, the type, number, and shape of FRCM layer. Both ultimate and yielding capacity decreased by 15 and 9%, respectively due to the erosion of the steel bar. Using PBO and carbon FRCM layer accomplished a great effect on improvement the ultimate strength of the corrosion damaged beams. The type, number, and the shape of FRCM layer had a large effect on failure shape and the ultimate capacity of the studied beams. Moreover, the influence of an innovative and efficient anchorage mechanism for improving the flexural capacity of RC beams reinforced with FRCM was discussed by Zena R. Aljazaeri et al. [13]. The influence of two anchorage systems (a glass spike and a U-wrapped anchor) on the failure of FRCM layer was discussed. The ultimate load increased by 24% when using two anchorage systems compared to beams without anchored mechanisms. Additionally, the U-wrapped PBO mechanism was more significant compared than the glass spike anchored system. Moreover, utilizing anchored U-wrapped PBO strip had a substantial influence on collapse mode. Where, the delamination failure of the PBO sheets converted into a slipping failure. Jacopo Donnini, et al, [14] presented an experimental and numerical analysis of FRCM behavior at high temperature. Depending on the type of fabric reinforcement used, FRCM systems can provide high temperature compatibility while maintaining mechanical performance when subjected to 120 C^o.

The major goal of this research is to provide a numerical parametric analysis by comparing the FEM results to those obtained from earlier experimental studies [10]. Moreover, presents several parameters study (main reinforcement ratio, number, type, and shape of FRCM layer). In addition, this research provides a suggested method to numerically assess the improvement of RC beams reinforced with FRCM. Additionally, provides the collapse mechanics of RC beams reinforced with FRCM.

2. METHODOLOGY

In this section, by using commercial FE software "ABAQUS", the attitude of full-scale RC beams reinforced with FRCM layer exposed to two concentrated static loads was discussed [15]. Moreover, all elements modeled as 3D finite elements. The material and geometric model that was used and modeling the bond behaviour between the FRCM layer and the concrete beam's soffit, are shown in Fig. 2. Both the cementitious mortar and the concrete parts were modelled as eight-node linear brick elements for the suggested finite element model. (C3D8R) [15]. Furthermore, the longitudinal and transverse bars were simulated using a two-node linear 3D truss element (T3D2). [15]. Also, the fabric textile was simulated as a 4-node doubly curved thin or thick shell (S4R) [15]. The mesh size was proposed by trying many different mesh sizes and comparing their results to decrease the run process time. Fig. 2 presents the FEM mesh details.

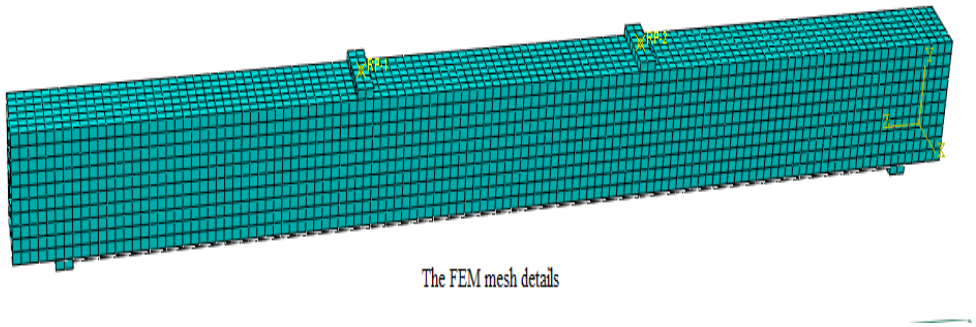

Fig.2 Details of 3D-FEM for discussed beams.

2.1. Concrete Model

For concrete, the efficient solution of the stiffness matrix is obtained using a FEM based on the Newton-Raphson iteration scheme for concrete. For modeling of RC elements under several load types like static, cyclic, monotonic, and dynamic loads, the concrete damaged plasticity (CDP) system in ABAQUS [16] is available. The (CDP) model allows simulating nonlinear compression behavior of concrete. The CDP variables are stated in Table 1. The Carreira and Chu model was used to simulate the concrete's stress-strain curve [17]. This model is extensively utilized to express simulate the concrete's stress-strain relationship. Until $0.4f_c'$, the concrete behaviour was expected to be elastic linear. The plastic behaviour occurs after this stage, according to Eq. (1).

$$f_c = f_c' \times \frac{\beta\,(\varepsilon/\varepsilon c\prime)}{\beta - 1 + (\varepsilon/\varepsilon c\prime)^{\beta}}, \quad (1)$$

Where f_c is concrete's uniaxial compressive stress, f_c' is concrete's typical uniaxial compressive strength, ε_c' is the concrete strain equivalent to f_c' and β is a material characteristic that depends on the form of the stress-strain curve and can be evaluated utilizing Eq. (2 and 3), and ε is the concrete's uniaxial compressive strain.

$$\beta = (f_c'/32.40)^3 + 1.55 \quad (2)$$

$$\varepsilon_c' = 0.002\ . \quad (3)$$

According to the Carreira and Chu model, concrete tension behaviour displays a straight increment until it reaches the ultimate tensile strength f_t' and then a linear softening till coming to zero. The concrete stress-strain curve in both tension and compression is seen in Fig. 3 (a). The greatest uniaxial tensile capacity may be evaluated from the following equation

$$f_t' = 0.10 \times f_c' \quad (4)$$

TABLE 1 DEFINED VARIABLES OF THE CONCRETE'S CDP MODEL. [16]

Parameter	Value
Concrete's compressive strength, $f_{c\prime}$ (MPa)	$f_{c\prime}$
Concrete's tensile strength, $f_{t\prime}$ (MPa)	$0.1f_{c\prime}$
Poisson's ratio, υ	0.15
Compressive damage variable, d_c	$1-(\sigma_c / f_{c\prime})$
Tensile damage variable, d_t	$1-(\sigma_t / f_{t\prime})$
Dilation angle,	35
Eccentricity, ε	0.1
Initial equibiaxial compressive yield stress divided by initial uniaxial compressive yield stress, (f_{bo} /f_{co})	1.16
Ratio of stress invariants, K	0.667
Viscosity Parameter, μ	0

2.2. Steel Model

The steel reinforcement's stress-strain relation was simulated as an elastic- perfectly plastic substance as seen in Fig. 3 (b). The material presents elastically linearly until coming the yielding point (f_y) with an elastic modulus

(200 GPa). The poison's ratio of the steel, which is equal to 0.3, is required by the FEM. The properties of steel in all examined beams at validation stage [10] and at parametric study stage are listed in Table 2.

TABLE 2 CONCRETE AND STEEL PROPERTIES USED IN DISCUSSED BEAMS

	Beam group	f_c' (N/mm^2)	f_t' (N/mm^2)	E_c (N/mm^2)	bar diameter		f_y (N/mm^2)	
					Tension zone	Comp-zone	Tension zone	Comp-zone
Validation Stage **[10]**	S1	23	2.3	28160	10	8	525.90	535.60
	S2	23	2.3	28160	12	10	515.44	521.89
Parametric study stage	B1	25	2.5	23500	12	10	360	360
	B2	25	2.5	23500	16	10	360	360
	B3	25	2.5	23500	22	10	360	360
	B4	25	2.5	23500	25	10	360	360
	B5	25	2.5	23500	25	10	360	360

Note: f_c' = Cylinder compressive concrete strength, f_t' = Tensile strength, E_c = Concrete's elastic modulus, and f_y = Yield strength of steel

2.3. Fabric Mesh Model

In the FEM, the FRCM-fabric textile was modeled as a 4-node doubly curved thin or thick shell (S4R). The stress-strain curve for fabric textile was represented as a linear-elastic material with brittle failure after coming to ultimate tensile capacity (fabric rupture), as seen in Fig. 3. (c). Table 3 shows the needed mechanical properties for defining the fabric textile in the FEM, like modulus of elasticity and ultimate capacity.

2.4. Cementitious Mortar Model

C3D8R [15] was utilized to simulate the cementitious mortar. Where, it's simulated as high strength concrete, with the same concrete's stress-strain curve as seen in Fig. 3 (a). Its mechanical properties are displayed in Table 3.

2.5. Bond-Slip Model

The bond behavior of FRCM materials has been examined in several earlier works [18-23]. Bond is in charge of achieving composite activity between the concrete and the FRCM layer. Bond has a large effect on the ultimate capacity and examined beam failure. Therefore, correctly simulating bond behavior is more important to define the accurate FEM. The bond behaviour was simulated utilizing Eq. (5 and 6) [18], which specified the cohesive interaction between concrete and the FRCM layer. This behavior is shown in Fig. 3 (d). The maximum friction stress (N_{max}) was assumed as (3 MPa). Furthermore, according to Luciano Ombres, [19], the displacement at damage initiation (δ_n^{intial}) and the displacement at damage failure (δ_n^{fail}) were considered to be (0.051mm) and (2.5 mm), respectively.

$$K_{nn} = \frac{N_{max}}{\delta_n^{intial}} \quad (5)$$

$$K_{nn\,(sof)} = \frac{N_{max}}{\delta_n^{fail} - \delta_n^{intial}} \quad (6)$$

where K_{nn} is the rigidity of the cohesion component in normal and $K_{nn\,(sof)}$ is the softening of cohesion component in normal.

TABLE 3 BOTH FRCM AND CEMENTITIOUS MORTAR PROPERTIES UTILIZED IN DISCUSSED BEAMS

property	Nominal thickness (mm)	Elastic modulus (GPa)	Tensile strength (MPa)	Tensile strain (%)	Compression strength (MPa)
PBO fiber mesh	0.0455 longitudinal 0.0224 transversal	270	5800	2.15	-
carbon fiber mesh	0.0455 longitudinal 0.0224 transversal	240	4800	2	-
Glass fiber mesh	0.0455 longitudinal 0.0224 transversal	80	2600	3.25	-

Mortar	3	6	3.50	-	29

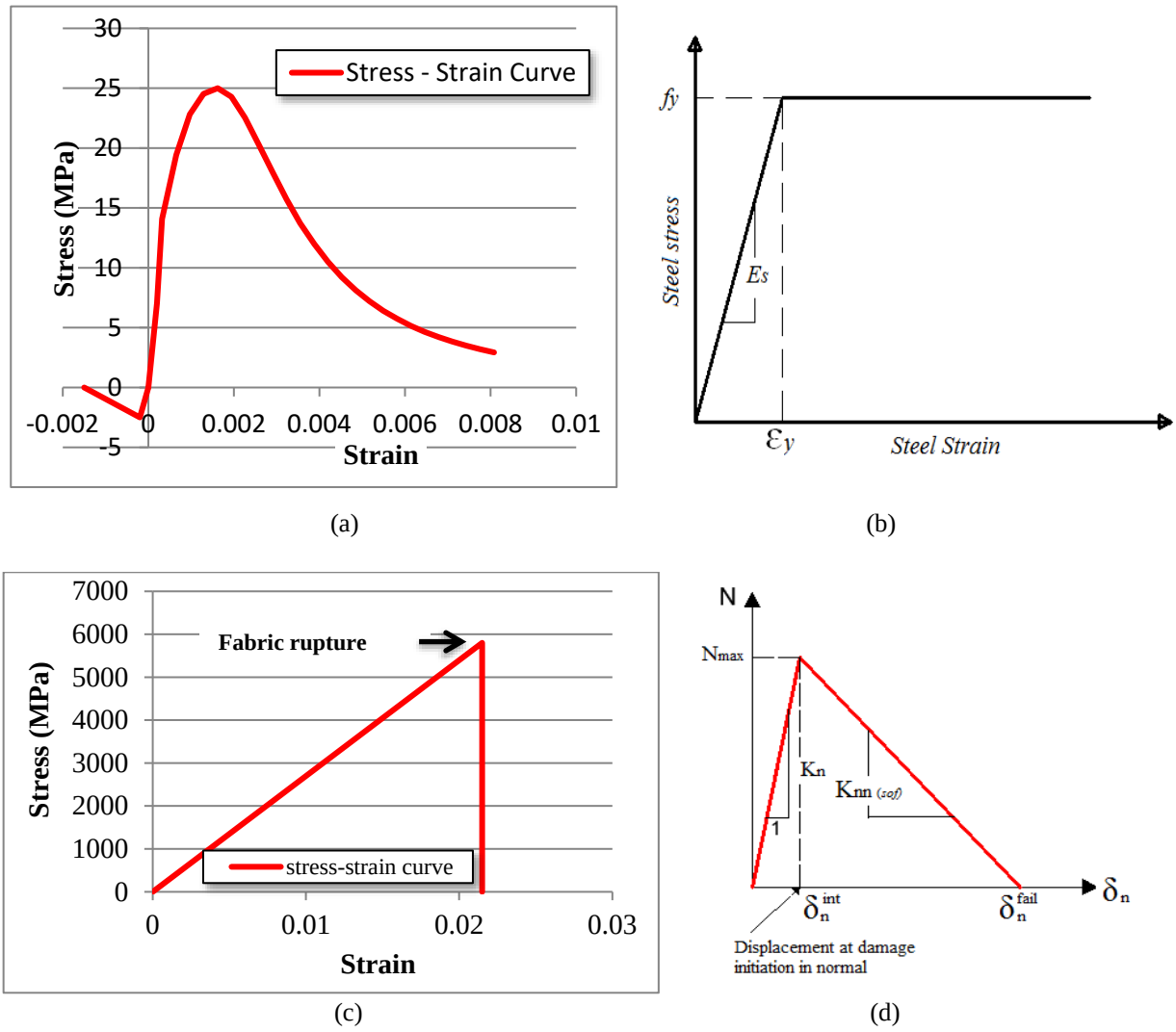

Fig.3 Material modeling: (a) Both concrete's tension and compression stress-strain curve, (b) Steel's stress - strain relationship, (c) Fabric textile's stress-strain relationship, (d) Separation - traction curve (sliding Mode).

3. VALIDATION OF THE FEM

To check the capacity of the developed FEM, the results which obtained from the previous experimental study [10] was compared with the predicted result obtained from the FEA. Validation was conducted in previous study [24]. The comparative results are detailed in the authors previous works [24].

3.1. Validation of Numerical Study

Fig. 4 shows the comparative of numerical and experimental load – deflection curves at mid span of the examined beams. This compression is between the commercial "ABAQUS results and the experimental results of Luciano Ombres, [10]. comparison between the cracking pattern, load – FRCM strain curves, and load – concrete strain curves at mid span of numerical and experimental results were discussed in authors previous works. The total previous experimental [10] and numerical results [24] showed a good validity of the FEM to present parametric study. So, the ABAQUS program can be used to do parametric study with high accuracy.

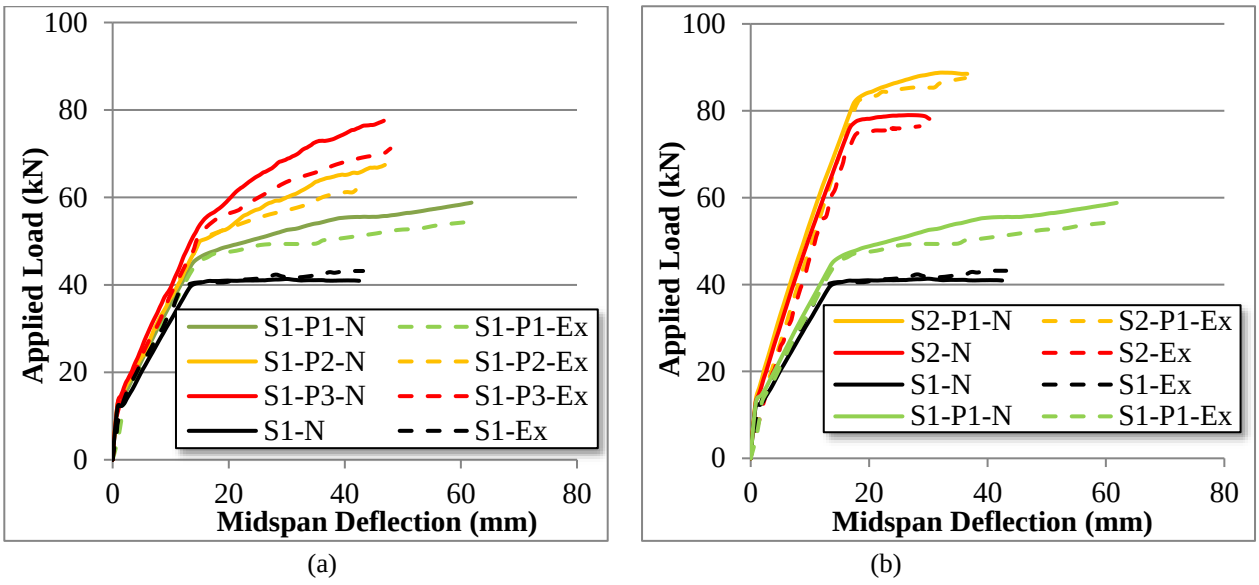

Fig.4 Comparative between experimental and numerical load – midspan deflection curves: (a) number of FRCM layer, (b) reinforcement ratio. (Validation stage) [10], [24].

4. NUMERICAL PARAMETRIC STUDY

4.1. Geometric Properties and Parameters

The examined beams have cross-section dimensional of 0.25× 0.70 m, simply supported with a total span of 7.0 m and clear span of 6.0 m as shown in Fig. 5. 19 beams were investigated and divided into five groups B1, B2, B3, B4, and B5. The considered main reinforcement ratio was 0.35%, 0.5%, 0.7%, 0.91%, and 1.2% for groups B1, B2, B3, B4, and B5, respectively to study the effect of reinforcement ratio. To prevent shear failure, all beams have one 8 mm stirrup every 12.5 cm as shear reinforcement, and have a 25 mm concrete cover, as seen in Fig. 5. Beams of groups B1, B2, B4 and B5 strengthened with one layer of PBO-FRCM, while beams of group B3 that strengthened with one, two and three layers of PBO, carbon, and glass FRCM to study the effect of number and type of FRCM layer. B3 strengthened with one layer of PBO-FRCM layer with U-wrapped shape to investigate the effect of FRCM shape. The properties of the examined beams in this parametric study were shown in Table 4. The rigid steel top-loading plates were subjected to two vertical focused loads. Similarly, two solid plates were modelled to represent the supporting points, with one constrained in both the (x and y) directions and the other only in the y direction Fig. 2.

The following parameters were investigated and analyzed in this work:

1. Main reinforcement ratio ($\mu = \frac{A_s}{b \times d}$), (0.35%, 0.5%, 0.7%, 0.91% and 1.2%)
2. Number of FRCM layer (one, two and three layer).
3. Type of FRCM layer (PBO, carbon and glass FRCM).
4. Shape of FRCM layer (straight FRCM and U-wrapped FRCM).

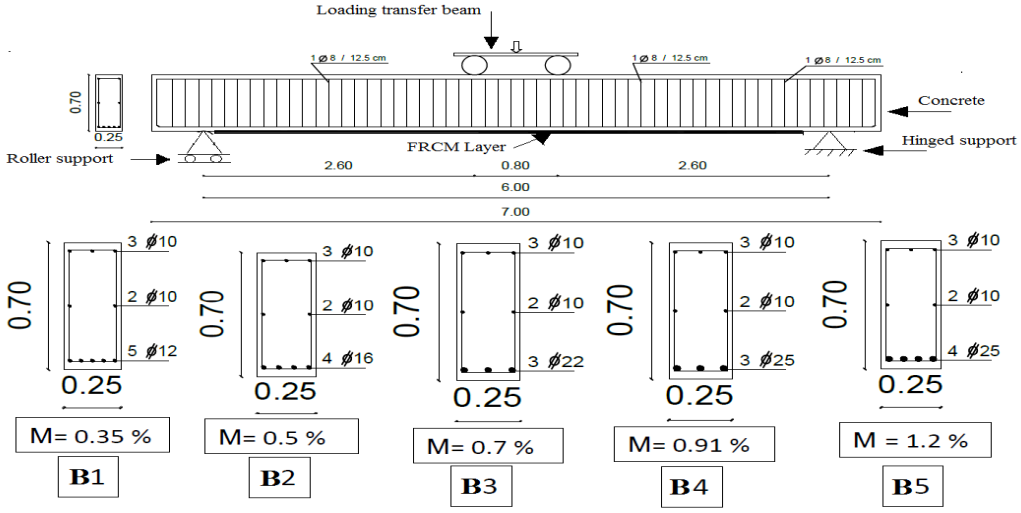

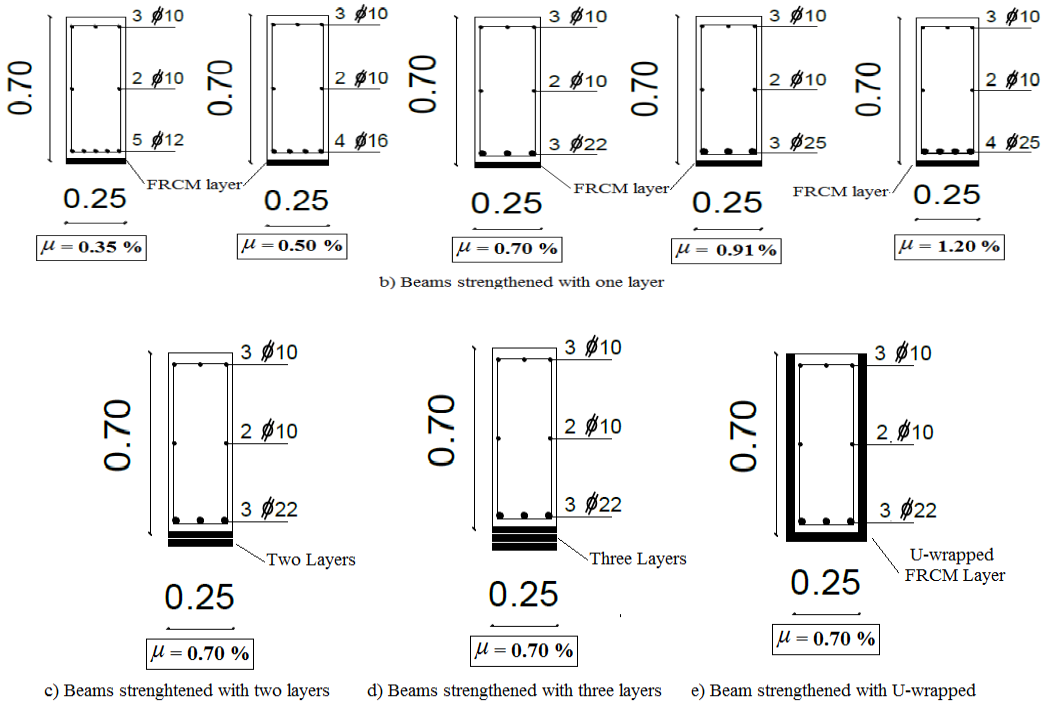

Fig.5 Analyzed investigated beams (parametric study stage).

TABLE 4 PROPERTIES OF THE INVESTIGATED BEAMS AT PARAMETRIC STUDY STAGE

Group number	Beam symbols	A_s (mm^2)	A'_s (mm^2)	A_f (mm^2)	Steel reinforcement		Fabric reinforcement ratio μ_f (%)
					μ (%)	α (%)	
B1	B1	565.49	235.62	-	0.35	0.42	0.000
	B1–P1	565.49	235.62	11.25	0.35	0.42	0.007
B2	B2	804.25	235.62	-	0.5	0.29	0.000
	B2–P1	804.25	235.62	11.25	0.5	0.29	0.007
B3	B3	1140.4	235.62	-	0.7	0.21	0.000
	B3–P1	1140.4	235.62	11.25	0.7	0.21	0.007
	B3–P2	1140.4	235.62	22.5	0.7	0.21	0.014
	B3–P3	1140.4	235.62	33.75	0.7	0.21	0.021
	B3–C1	1140.4	235.62	11.25	0.7	0.21	0.007
	B3–C2	1140.4	235.62	22.5	0.7	0.21	0.014
	B3–C3	1140.4	235.62	33.75	0.7	0.21	0.021
	B3–G1	1140.4	235.62	11.25	0.7	0.21	0.0069
	B3–G2	1140.4	235.62	22.5	0.7	0.21	0.014
	B3–G3	1140.4	235.62	33.75	0.7	0.21	0.021
	B3–P1 U-wrapped	1140.4	235.62	11.25	0.7	0.21	0.007
B4	B4	1472.62	235.62	-	0.91	0.16	0.000
	B4–P1	1472.62	235.62	11.25	0.91	0.16	0.007
B5	B5	1963.5	235.62	-	1.2	0.12	0.000
	B5–P1	1963.5	235.62	11.25	1.2	0.12	0.007

Note: The following labels were used to categorize the beams: the first letter ‘‘B’’ and the first number (1, 2, 3, 4, and 5) denote the group of the discussed beams (B1, B2, B3, B4, and B5); the second letter denotes FRCM type applied to the concrete surface, while the last number (1, 2, and 3) denotes FRCM number applied to the discussed beams. Finally, (U-wrapped) refers to the shape of FRCM layer.

4.2. Numerical Results and Discussion

The FEM data pertinent to this work is detailed and studied in the following sections, the acquired numerical results listed in Table 5.

TABLE 5 FEM RESULTS FOR PARAMETRIC STAGE

Group number	Beam designation	P_{Cr} (kN)	P_y (kN)	P_U (kN)	P_f (kN)	δ_y (mm)	δ_f (mm)	Failure mode
B1	B1	69.04	127.70	139.32	135.10	13.05	79.54	DFF
	B1–P1	71.01	133.30	168.32	168.32	13.20	67.32	DFF
B2	B2	72.95	166.28	178.28	174.03	14.25	58.19	DFF
	B2-P1	76.15	170.00	204.46	204.46	14.51	56.98	DFF
B3	B3	78.9	220.53	234.45	229.80	16.13	45.73	DFF
	B3-P1	83.6	227.57	254.43	254.43	16.77	43.56	DFF
	B3-P2	84.98	239.12	268.28	268.28	18.56	38.69	IC
	B3-P3	86.89	245.26	277.82	277.82	18.68	37.00	IC
	B3-C1	83	227.40	252.95	252.95	16.84	44.24	DFF
	B3-C2	83.89	236.63	266.01	266.01	19.22	39.79	IC
	B3- C3	84.4	242.72	276.84	276.84	18.63	37.93	IC
	B3-G1	81.9	221.29	243.46	241.72	15.86	47.01	DFF
	B3-G2	83.65	225.67	249.3	248.60	16.01	44.71	IC
	B3-G3	84.05	229.80	256.34	256.34	16.47	40.46	IC
	B3–P1 U-wrapped	87.07	247.54	294.04	294.04	15.47	37.73	DFF
B4	B4	83.3	270.58	288.4	283.45	16.99	41.75	DFF
	B4-P1	86.85	275.84	304.39	303.47	17.70	40.26	DFF
B5	B5	86.22	345.86	363.2	353.89	18.71	38.72	DFF
	B5-P1	89.67	348.34	376.62	371.67	19.06	37.71	DFF

Note: P_{Cr} = Cracking load, P_y = yielding load, P_U = Ultimate load, P_f = failure load, δ_y = Deflection at yielding load; δ_u = Deflection at failure load, DFF = Ductile flexural failure, IC = Intermediate crack debonding.

4.2.1. Effect of Main Reinforcement Ratio

4.2.1.1. Load Deflection Curve

Fig. 6 displays the influence of main reinforcement ratio on load-midspan deflection curve. For all of the examined RC beams, the behaviour reveals three steps from the starting of loading to failure. The primary one is cracking stage, which is almost same in all beams. The reason can be proved as that all beams have nearly identical concrete cross-section dimensions and properties. While the second one is the cracked stage (pre-yielding phase) begins when the concrete cracks and continues until the steel yields. The inclination of the line decreases because of the propagating cracks along the investigated beams, indicating a decrease in stiffness. Furthermore, a significant gradient shows that the beam is stiff at this stage. Though the final stage is the post-yielding phase, where the cracks grow and number, the deflection increases with a minor increase in load. Because the rigidity of the tested beams is deteriorating, the incline of the curves appears as a semi-horizontal line. Moreover, it can be inferred that utilizing PBO – FRCM leads to increasing the serviceability of the examined beams.

4.2.1.2. Cracks ultimate and failure loads

Fig. 7 (a) shows the relation between main reinforcement ratio and failure load. Additionally, it can be concluded that when the reinforcement ratio is low, utilizing the FRCM system is more significant than utilizing the reinforcement ratio is high. Where, the percentage of the increasing in failure load was 25 % and 5 % for low (0.35%) and high (1.2%) reinforcement ratio, respectively. Fig. 7 (b) shows the relation between main reinforcement ratio (μ) versus cracking and ultimate load. As displayed in Fig. 7 (b), raising the reinforcement ratio (μ), improves the cracking and ultimate load of the investigated beams. Where, utilizing PBO – FRCM leads to increasing the ultimate load by 21 % and 3.4 % for low (0.35%) and high (1.2%) reinforcement ratio, respectively.

4.2.1.3. Cracks Pattern and Strain Distribution

Fig. 8 (a) and Fig. 8 (b) show the influence of reinforcement ratio on the strain distribution and cracking pattern at failure load. As shown in Fig. 8 (a), the beams without any strengthened FRCM layer showed more localized crack pattern area. The maximum strain occurred at the soffit of the beam. The cracks clearly started from the same area of maximum strain. Whereas, the beams reinforcement with one layer of PBO- FRCM were noted that

the cracks occurred in a wide area compared with the beams without strengthening. Moreover, the maximum strain occurred at the middle of the examined beams and the cracks started from the same place as shown in Fig. 8 (b). This can be attributed to the PBO- FRCM layer that played as extra reinforcement to reduce the strain and restrict the cracks.

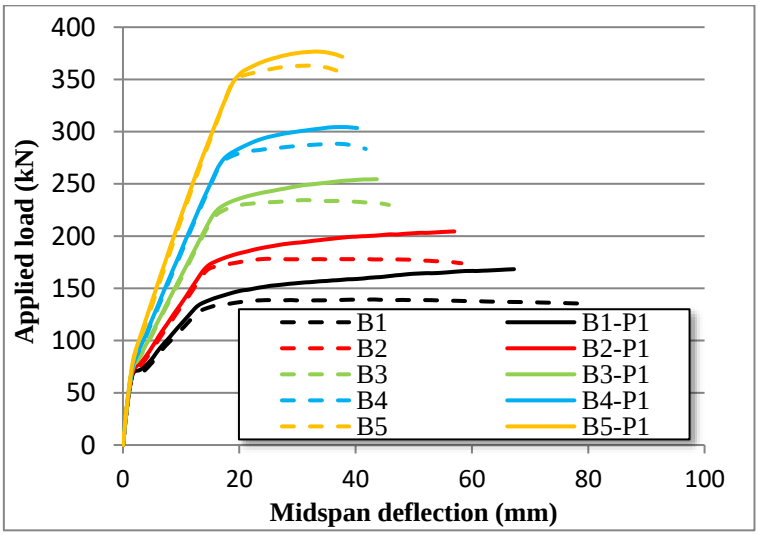

Fig.6 Effect of reinforcement ratio μ (%) on load- midspan deflection curves

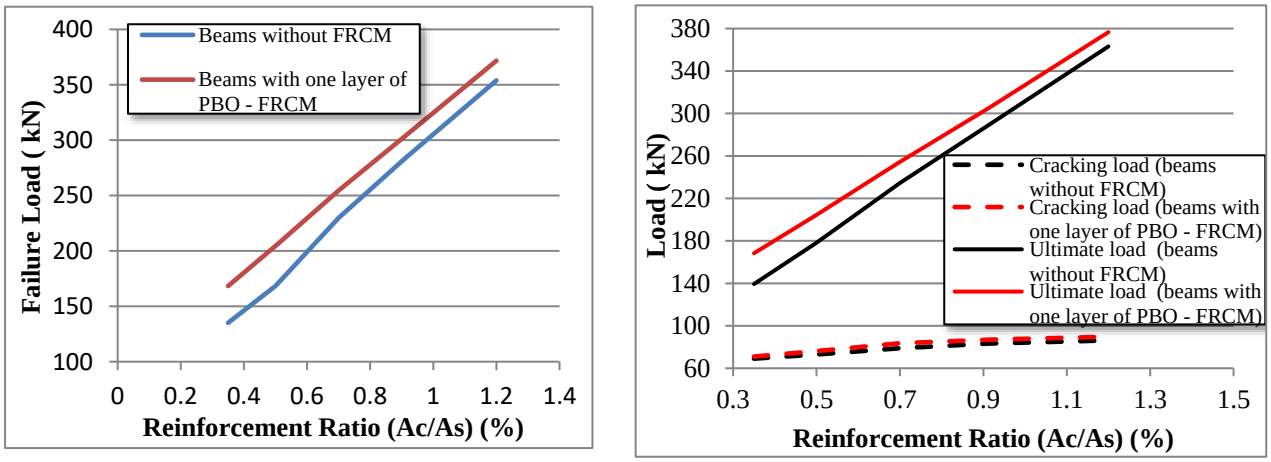

(a) (b)

Fig.7 The relation between Reinforcement ratio μ (%) and: **(a)** failure load (KN), **(b)** both cracking and ultimate loads.

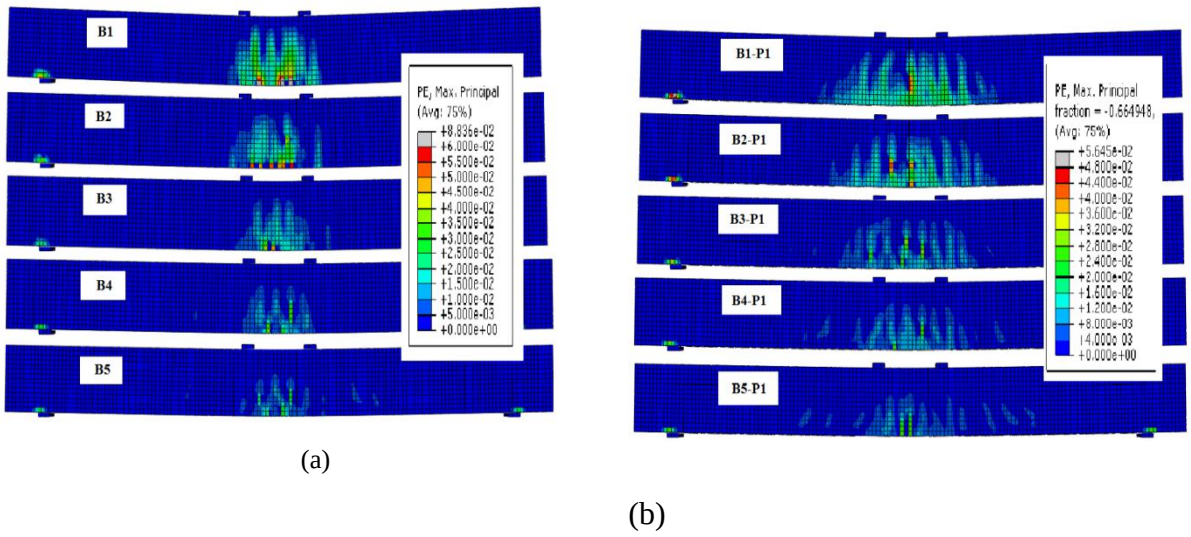

(a)

(b)

Fig.8 Effect of reinforcement ratio μ (%) on the strain distribution and cracking pattern: (a) (beams without FRCM layer), (b) (beams with one layer of PBO-FRCM).

4.2.1.4. Strain of FRCM Layer and Concrete

Fig. 9 (a) displays the load–PBO FRCM strain measured at mid span. The load against concrete strain recorded at mid-span for all discussed beams are displayed in Fig. 9 (b). The positive strain value in the FRCM system pointes to the tension strain, whereas the negative strain value in concrete pointes to the compressive strain. Each load-midspan strain curve is made up of three straight lines with various inclinations like load-midspan deflection curves. Fig. 9 (a) displays the influence of reinforcement ratio on the PBO- FRCM strain measured at mid span. In comparison to beams with a high reinforcement ratio, those with a lower reinforcement ratio had greater PBO-FRCM strain values. This is because raising reinforcement causes decrease the reinforcement stress and an increasing of the beam rigidity, hence stiffer behavior is prominent and make beams stiffer. Fig. 9 (b) displays the influence of reinforcement ratio on the compressive concrete strain measured at mid span. The compressive concrete strain decreases at the same load by increasing the reinforcement ratio. The reason can be described as that the decreasing of reinforcement ratio causes an increasing of their tensile stress. This results an increasing of tensile and compressive strain in the reinforcing bars and top layer of concrete, respectively.

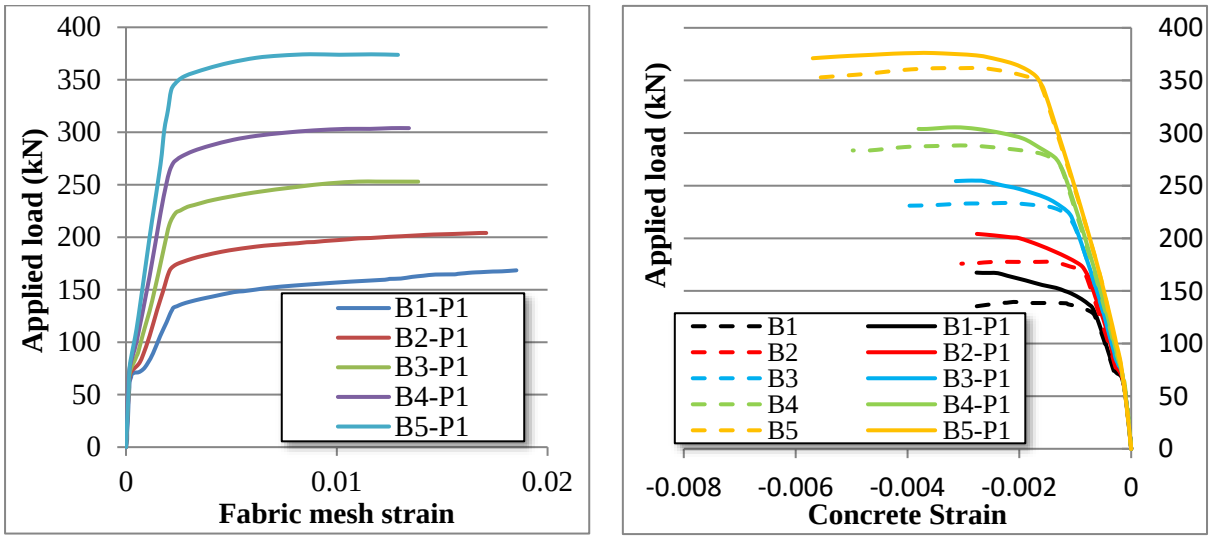

(a) (b)

Fig.9 Effect of reinforcement ratio μ (%) on: (a) fabric mesh strain curves at mid span, (b) concrete strain curves at mid span.

4.2.2. Effect of Number of FRCM layer

4.2.2.1. Load Deflection Curve

Fig. 10 shows the influence of increasing number of FRCM layer on load-midspan deflection. Clearly, there is major improvement in the serviceability of the examined beams strengthened with more than one layer. The increment of FRCM layers, however, plays as an additional reinforcement for the studied beams, accordingly, the ductility of the examined beams was reduced. Fig. 11 (a) shows the number of layers versus failure load. Fig. 11 (a) shows that utilizing one layer of FRCM is more significant than utilizing two or three FRCM layers. This is due to that failure of the beams with one layer of FRCM proceeded with concrete crushing. Whereas, the beams used two or three layers of FRCM collapsed as debonding FRCM layers. This means that the strengthened beam not taking full advantage of strengthening layers.

4.2.2.2. Cracks ultimate and failure loads

Fig. 11 (a) shows that utilizing of one layer of glass, Carbon and PBO FRCM increasing the failure load by 5.18%, 10.07% and 10.71% respectively. While utilizing of two layers of glass, carbon and PBO FRCM increase the failure load by 8.18%, 15.75% and 16.74% respectively. Finally, the failure load increased by 11.5%, 20.47% and 20.90% when using three layers of glass, Carbon and PBO FRCM. Moreover, Fig. 11 (b) shows the relation between number of FRCM layers versus cracking and ultimate load. Where, increasing number of FRCM layers causes increase the cracking and ultimate capacity of the investigated beams as shown in Fig. 11 (b).

4.2.2.3. Cracks Pattern and Strain Distribution

Fig. 12 shows the influence of increasing number of FRCM layers on strain distribution and cracking pattern at failure load by utilizing different three types of FRCM layers (PBO, Carbon and Glass). The Figures display that the cracks opening of the analyzed beams were restricted when the number of FRCM layers increased.

Moreover, it is clear that the increasing number of FRCM layers resulted in converting the cracking zone from localized cracking to wide cracking area. The reason for this is that the increasing number of FRCM layers played as extra reinforcement for the examined beams.

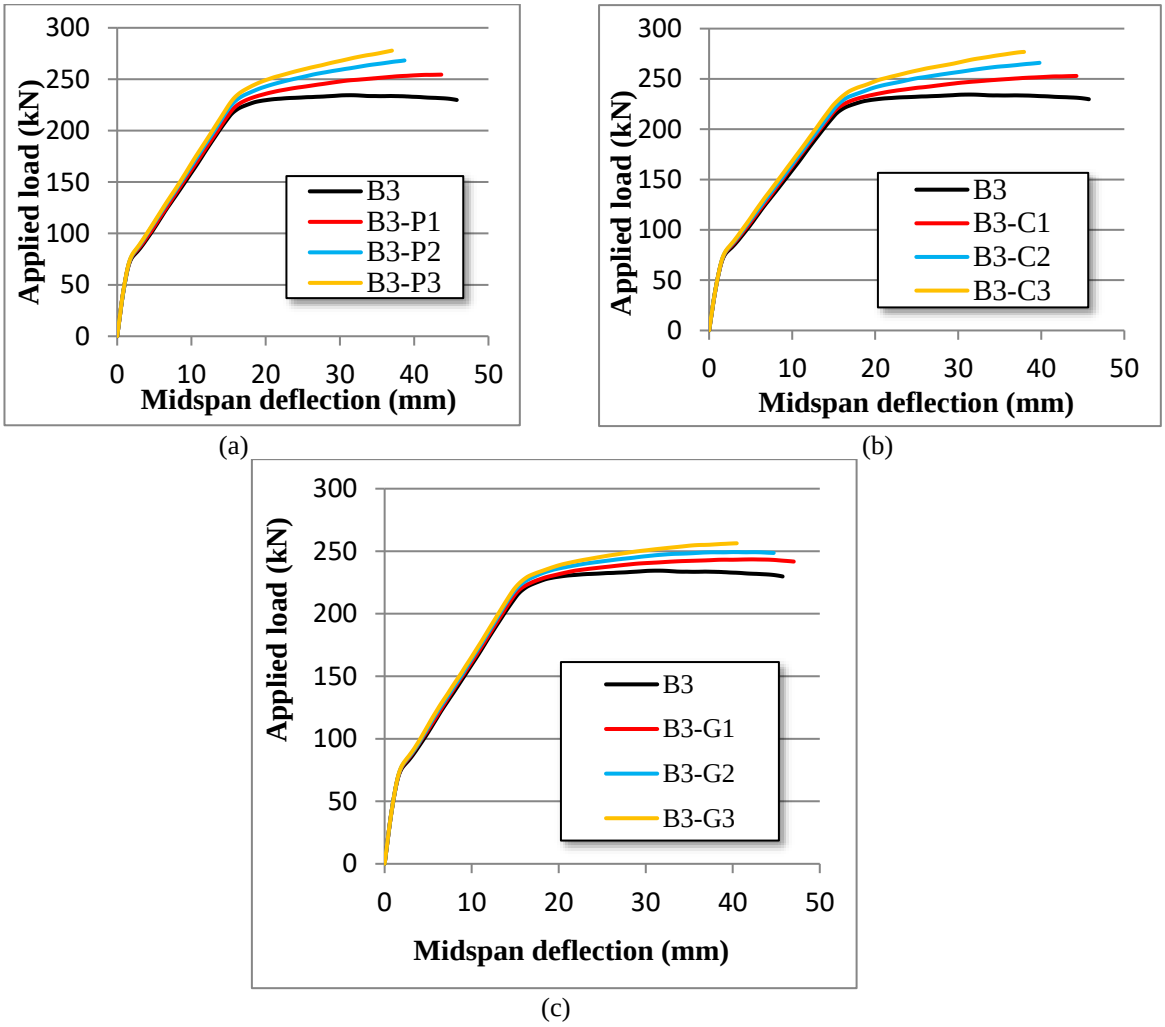

Fig.10 Effect number of FRCM layer on load- midspan deflection curves: (a) using PBO - FRCM layer, (b) using carbon - FRCM layer, (c) using glass - FRCM layer.

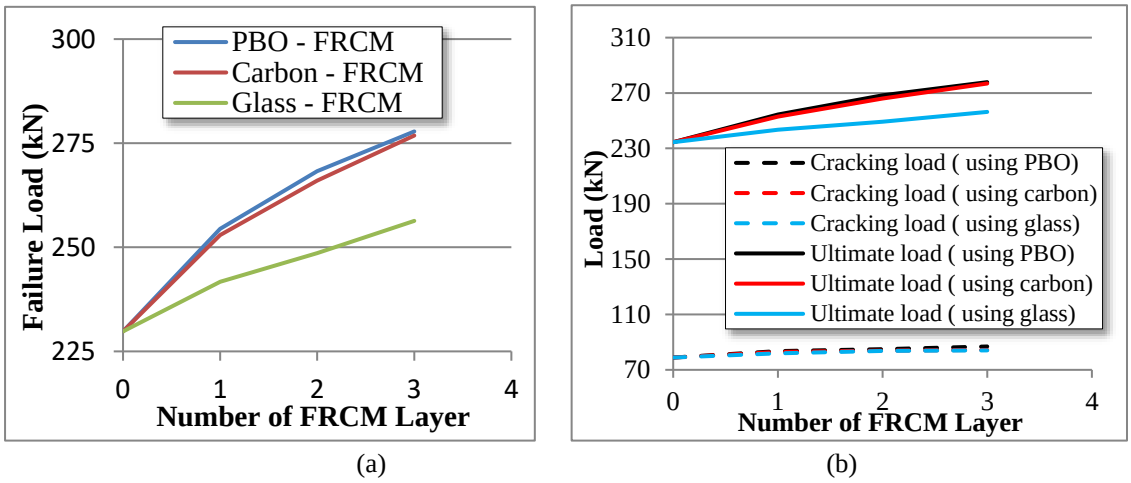

Fig.11 The relation between number of FRCM layer and: (a) failure load (KN), (b) both cracking and ultimate loads.

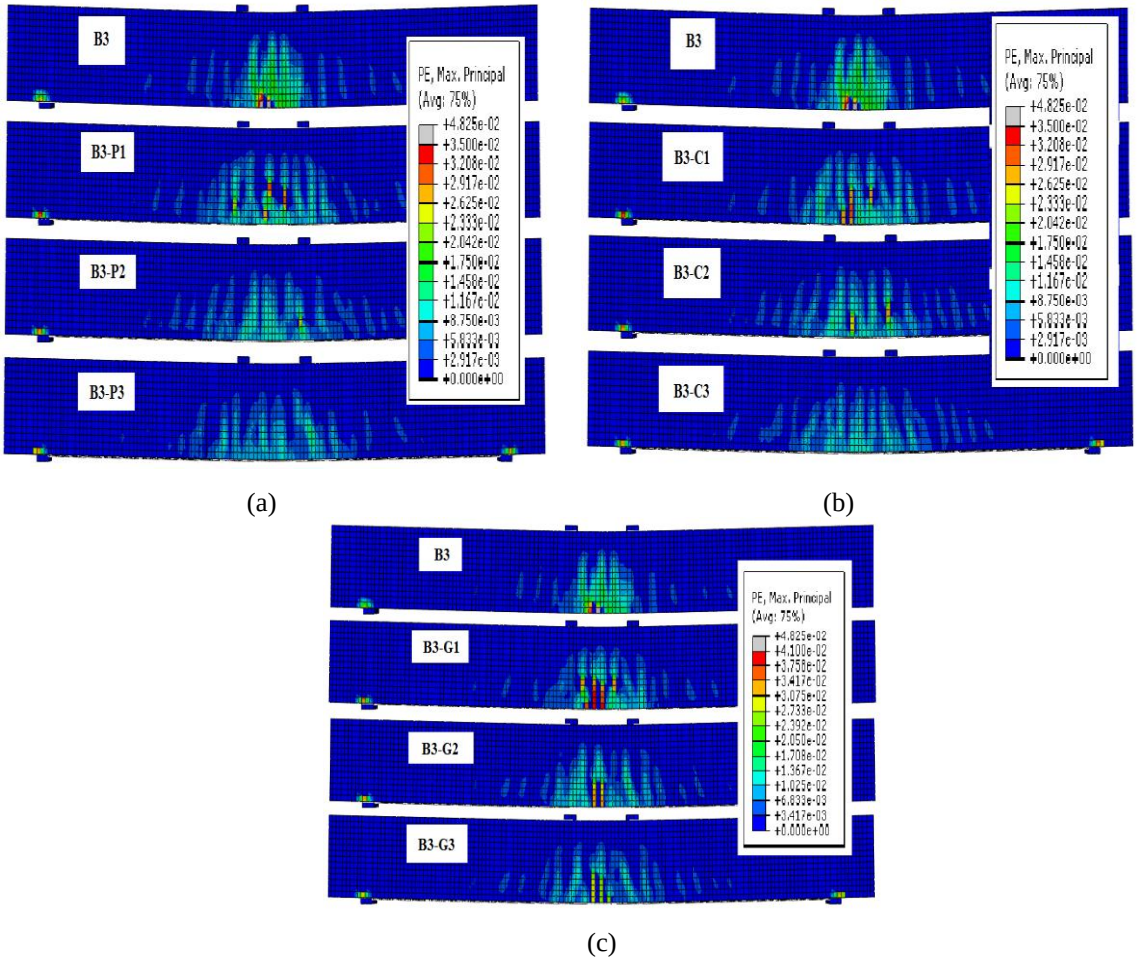

(a) (b)

(c)

Fig.12 Effect number of layers on strain distribution and cracking pattern: (a) using PBO - FRCM layer, (b) using carbon - FRCM layer, (c) using glass - FRCM layer

4.2.2.4. Strain of FRCM Layer and Concrete

Fig. 13 (a) shows the influence of increasing number of FRCM layers on their strain at midspan. The beams with one layer of FRCM present higher strain values compared with the beams used two or three layers. A significant increase of the FRCM strain at the midspan was noticed after the steel yielding. Fig. 13 (b) shows the influence of increasing number of FRCM layers on compression concrete strain measured at midspan. At failure, the compression strain of the concrete varies between 0.004 and 0.003 mm/mm for unstrengthened beams and strengthened with one layer of FRCM, respectively. For the examined beams strengthened with two or three layers, their strain at failure was ranging in the interval 0.0029 mm/mm and 0.0026 mm/mm.

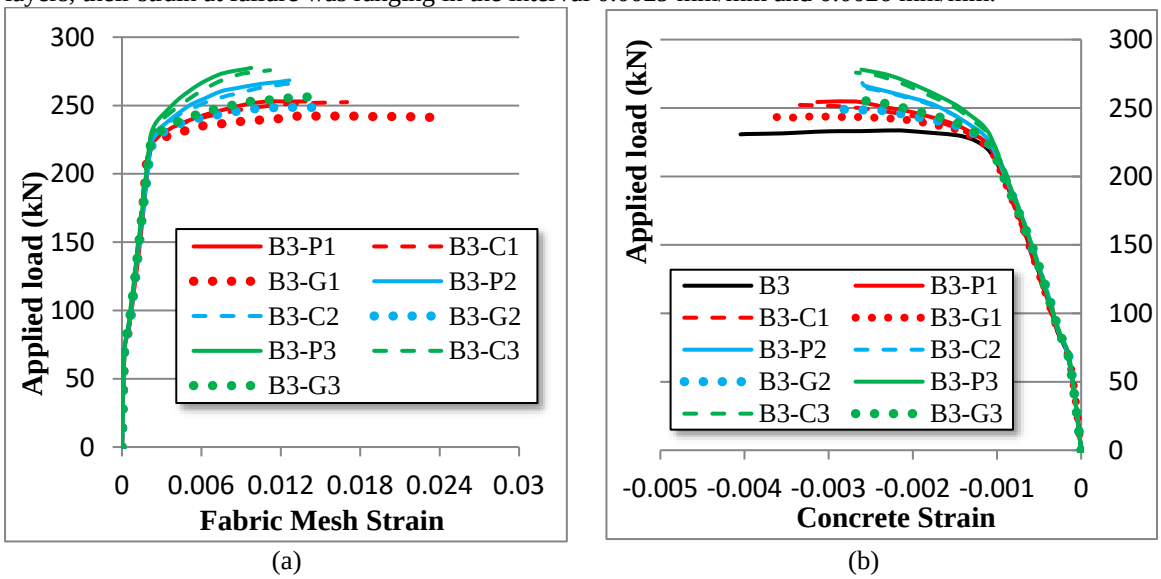

(a) (b)

Fig.13 Effect number and type of FRCM layers: (a) fabric mesh strain curves at mid span, (b) concrete strain curves at mid span.

4.2.3. Effect Type of FRCM layer

4.2.3.1. Load Deflection Curve

Fig. 14 displays the influence of FRCM type on the load–midspan deflection curves. These figures demonstrate the contributing of the FRCM in resisting the applied loads after yielding of the main reinforcement. Utilizing glass and PBO of FRCM layers increased the failure load of the examined beams by 5% to 11%, respectively compared with the control beams. Fig. 15 (a) shows the effect of type of layer versus the failure load. It can be noticed the beams strengthened with PBO-FRCM or carbon-FRCM had the same the ultimate load capacity. The reason for this is that the rapprochement of PBO and carbon FRCM in mechanical properties. On the contrary, neither utilizing glass FRCM layers given a noticeable increase in the failure load compared the control beam. Moreover, Fig. 15 (b) shows the relation between type of FRCM layers versus cracking and ultimate load. Where, usage of PBO- FRCM layers had a significant effect on the cracking and ultimate load of the investigated beams compared with utilizing carbon and glass FRCM as shown in Fig. 15 (b).

4.2.3.2. Cracks Pattern and Strain Distribution

Fig. 16 shows the influence of type of FRCM layers on strain distribution and cracking pattern at failure load. PBO FRCM layer is more efficient compared with the other two types of FRCM layers. Utilizing PBO FRCM layers leads to restrict the propagated cracks. Moreover, the cracks spread in wide zone and maximum strain occurred at the middle of the examined beams when using PBO and carbon FRCM layers. On the other hand, when utilizing glass FRCM layers, the cracks spread in almost localized zone area and maximum strain occurred at the of cross section.

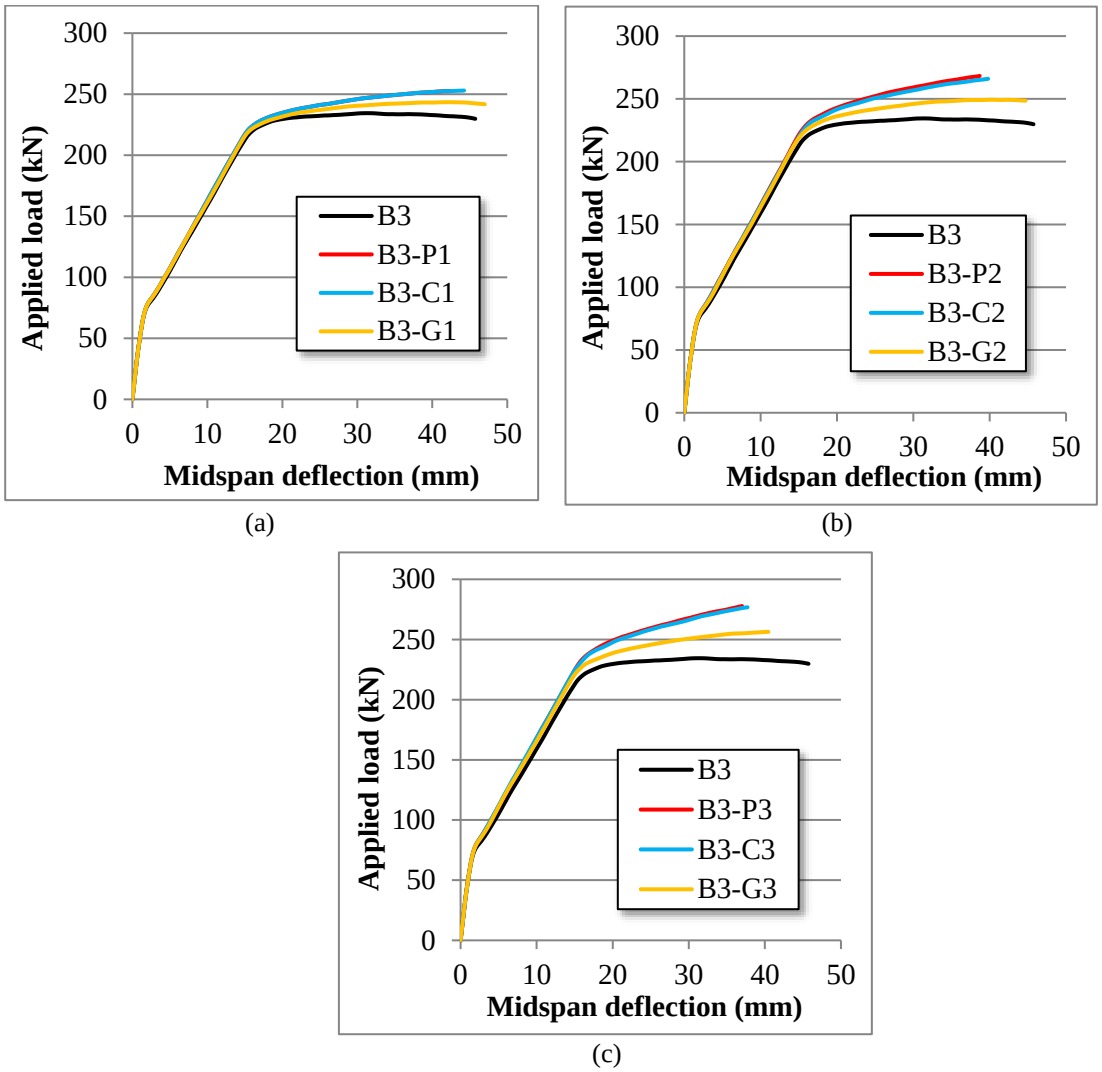

Fig.14 Effect type of FRCM layer on load- midspan deflection curves: (a) using one layer, (b) using two layers, (c) using three layers.

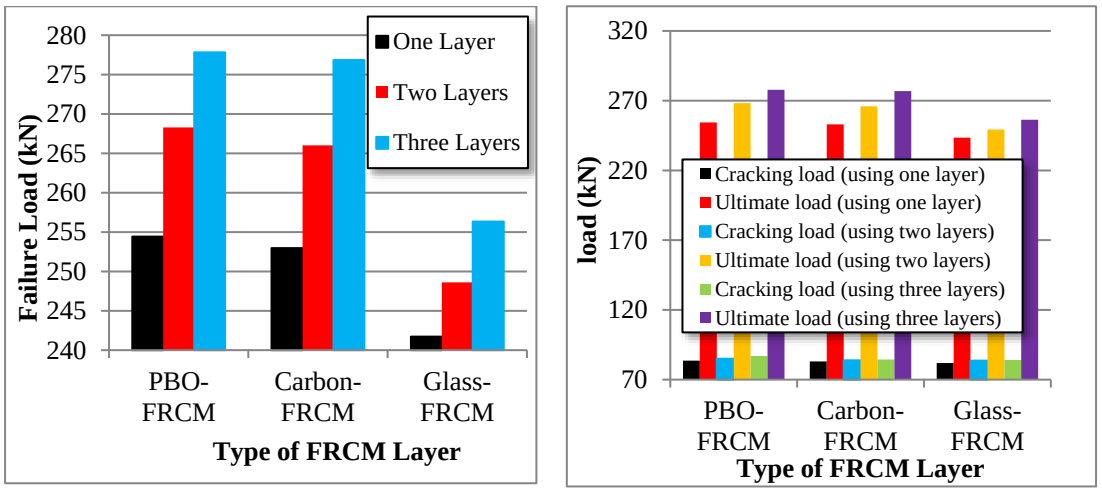

Fig.15 The relation between type of FRCM layer and: (a) failure load (KN), (b) both cracking and ultimate loads.

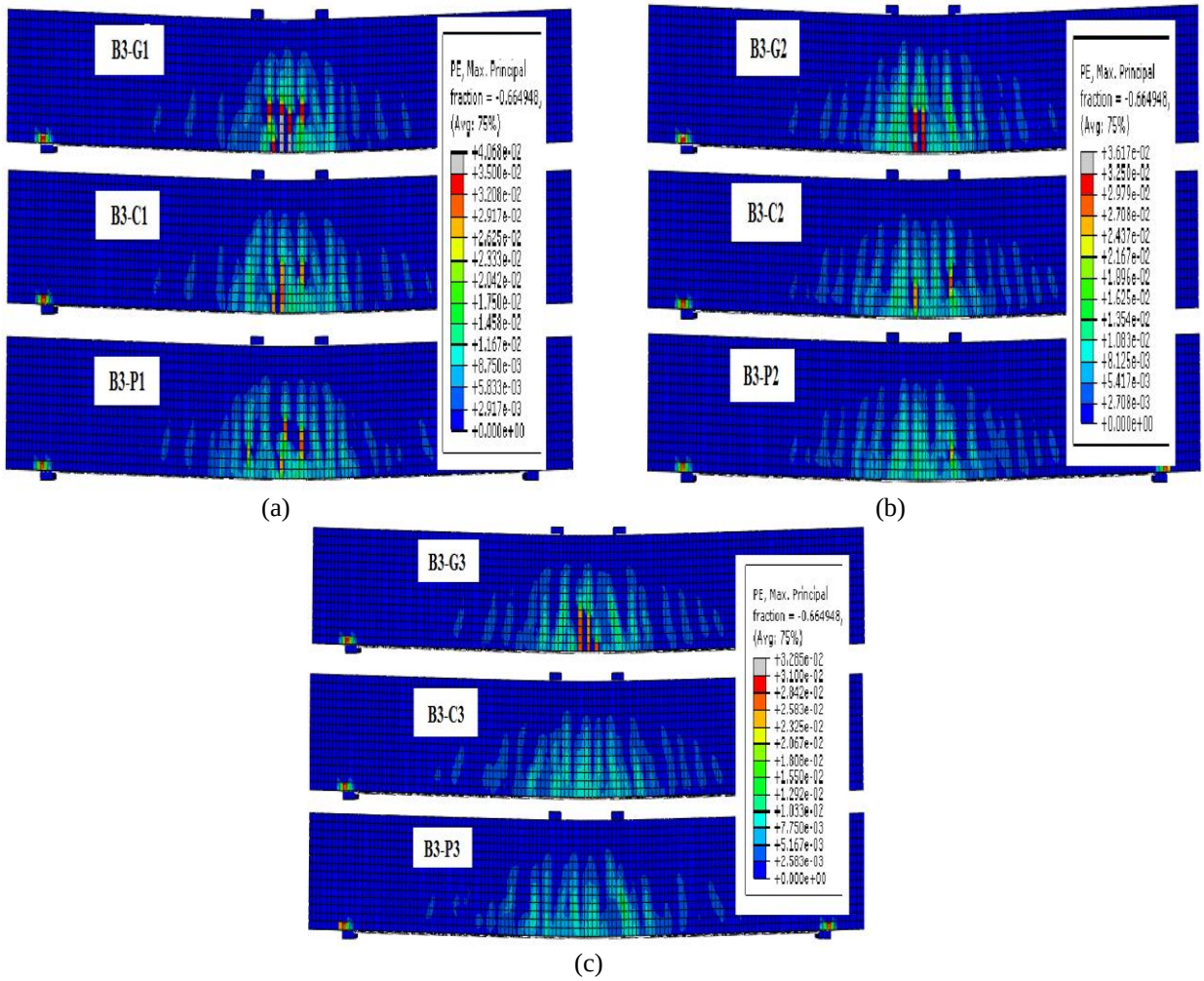

Fig.16 Effect type of layers on strain distribution and cracking pattern: (a) using one layer, (b) using two layers, (c) using three layers.

4.2.3.3. Strain of FRCM Layer and Concrete

Fig. 13 (a) also shows the type of FRCM layers verses FRCM layers strain measured at mid span. Utilizing PBO and carbon FRCM layers made the examined beams stiffer than using glass FRCM layers. Therefore, low strain value was recorded when using glass FRCM compared with utilizing PBO and carbon FRCM which recorded high strain value. Fig. 13 (b) shows the type of FRCM layers verses compression concrete strain measured at mid span. The figure also revealed that utilizing PBO FRCM more significant than using other types.

4.2.4. Effect Shape of FRCM layer

4.2.4.1. Load Deflection Curve

Fig. 17 displays the shape influence of FRCM layer on load–midspan deflection curve. Utilizing of U-shaped FRCM layer was more efficient in increasing the capacity load. Moreover, using U-shaped FRCM layer was more effective than straight FRCM layer as shown in Fig. 18 (a). U-shaped FRCM layer achieved an increasing in the failure load by 28% compared with the control beam. On the other side, the straight FRCM layer (B3-P1) only increased the failure load by 11% compared with the control beam. The reason for this is that the two sides of the U-shaped FRCM layer worked as extra flexural reinforcement compared with the straight FRCM layer. Moreover, Fig. 18 (b) shows the relation between shape of FRCM layers versus cracking and ultimate load. Where, usage of U-shaped layer had a significant effect on the cracking and ultimate load of the investigated beams compared with straight FRCM layer as shown in Fig. 18 (b).

4.2.4.2. Cracks Pattern and Strain Distribution

Fig. 19 shows effect of FRCM shape on strain distribution and cracking pattern at failure load of the investigated specimens. Utilizing U-wrapped FRCM layer strengthened the examined beams and made the beam stiffer. Moreover, the cracking zone widely propagated when using U-wrapped FRCM compared with using straight FRCM layer.

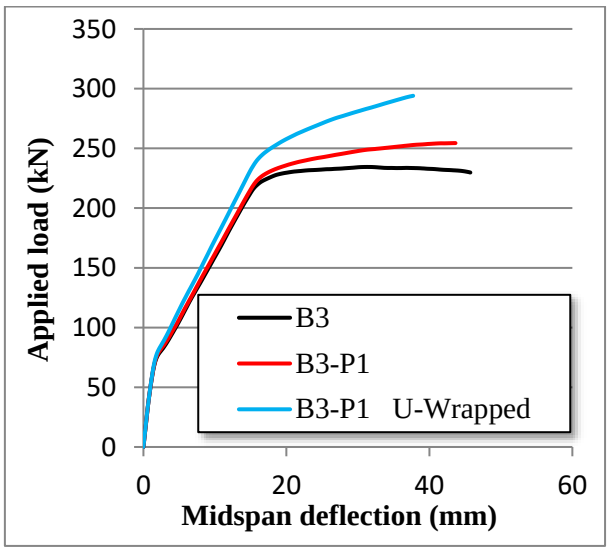

Fig.17 Effect shape of FRCM layer on load- midspan deflection curves (using one layer)

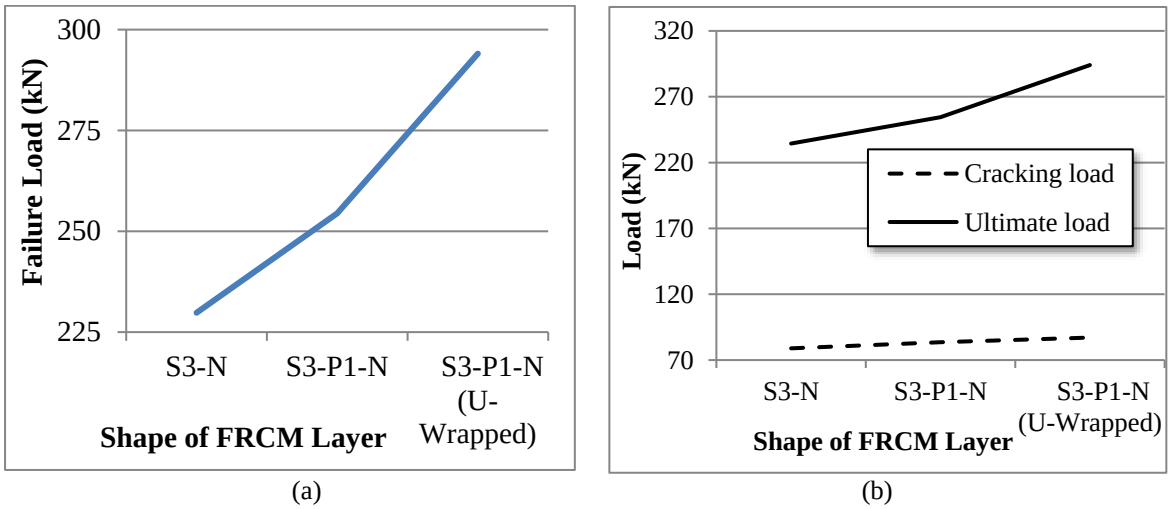

(a) (b)

Fig.18 The relation between shape of FRCM layer and: (a) failure load (KN), (b) both cracking and ultimate loads.

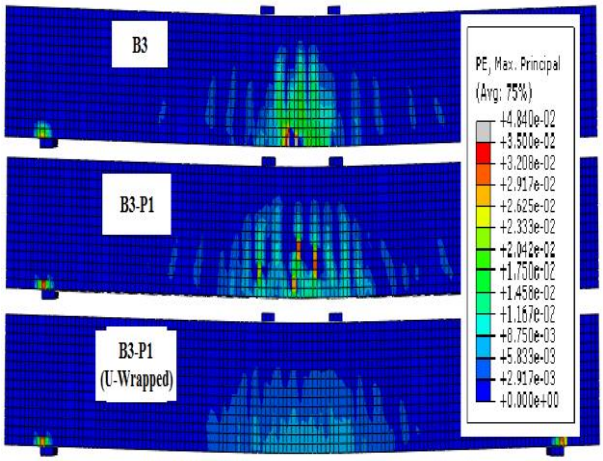

Fig.19 Effect shape of FRCM layer on strain distribution and cracking pattern (using one layer).

4.2.4.3. Strain of FRCM Layer and Concrete

Fig. 20 (a) shows the shape effect of FRCM layers verses FRCM layers strain measured at midspan. Usage U-wrapped FRCM layer had a significant effect on the recoded PBO-FRCM strain. At the same load, utilizing U-wrapped PBO-FRCM layer had lower stain value compared with using straight PBO-FRCM layer. Fig. 20 (b) shows the shape effect of FRCM layers against compression concrete strain measured at mid span. Clearly, using U-wrapped PBO-FRCM layer leads to decrease compression concrete strain value compared with utilizing straight PBO-FRCM layer.

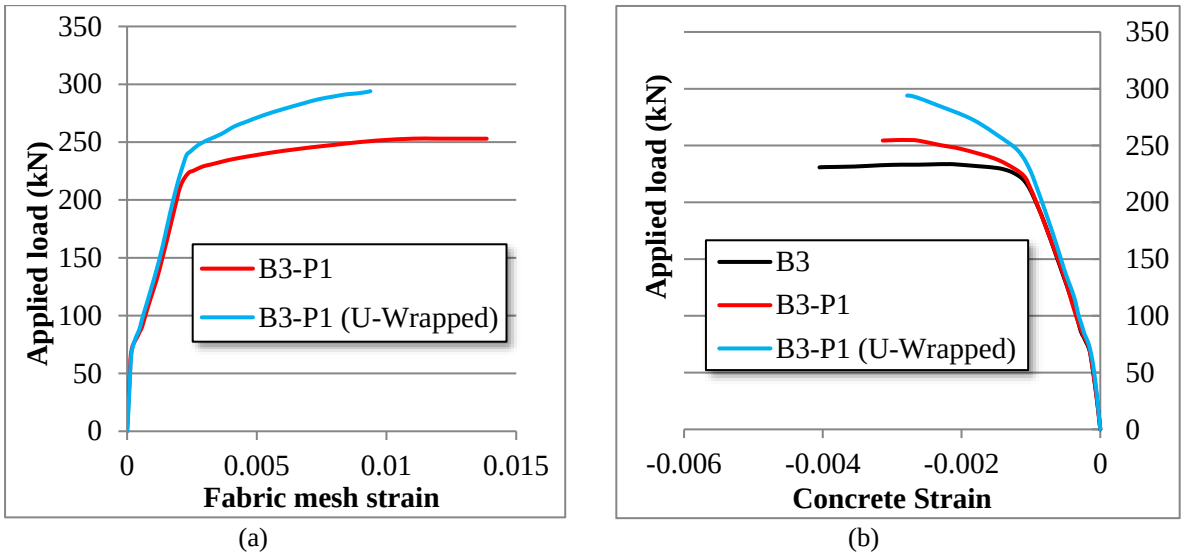

Fig.20 Effect shape of FRCM layers: (a) fabric mesh strain curves at mid span, (b) concrete strain curves at mid span.

4.3. Failure mode

From previous studies, [10-14] it can be noticed that the type of failure mode had a significant effect when utilizing FRCM layers. The results obtained in our study support the previous studies, since adding more FRCM layers changed the failure mode. The failure mode for beams without strengthened (B1, B2, B3, B4 and B5) and beams strengthened with one layer of FRCM (B1-P1, B2-P1, B3-P1, B4-P1, B5-P1, B3-C1, B1-G1 and B1-P1 (U-wrapped) occurred due to yielding of steel followed by crushing of concrete in compression side (Ductile flexural failure) as shown in Fig. 21 (a). Whereas intermediate debonding failure for beams used two or three FRCM layers (B3-P2, B3-P3, B3-C2, B3-C3, B3-P1, B3-G2, B3-G3) was observed, as shown in Fig. 21 (b). Moreover, Fig. 21 (c) shows shear stress on the upper surface of the FRCM layer. High shear stress indicates the area in which debonding occurs. This proved that the failure mode depends on the number of FRCM layers.

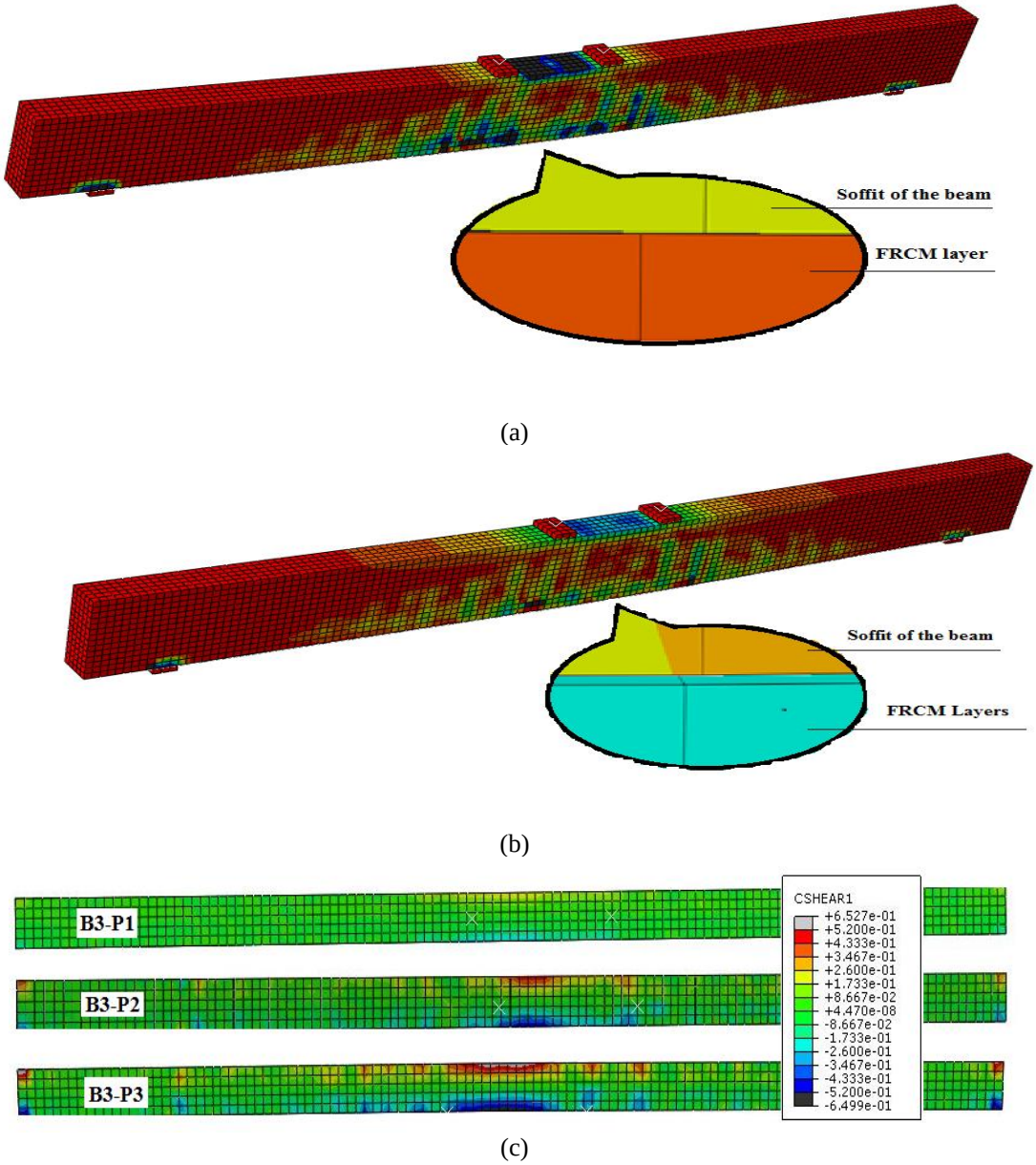

Fig.21 Type of failure mode: (a) Ductile flexural failure, (b) Debonding of FRCM layers, (c) Shear stress on the top surface of FRCM layer (interaction between concrete and FRCM layers).

5. CONCLUSION

To modeled RC beams reinforced with FRCM, a finite-element analysis was performed. For six reinforced large-scale RC beams, the simulation was compared to **Luciano Ombres'** experimental results **[10]**. Nineteen large-scale RC beams were used to study number of parametric study. Based on the presented analysis, the following concluding remarks were mentioned:

1- In terms of stiffness, deformation capacity, and strength, the FEA a good validation with the experimental response of the simulated beams.
2- Using FRCM system improved the flexural strength of reinforced beams. The failure load of strengthened beams increased by 28% compared with the un-strengthened beam.
3- Using FRCM system is more significant in case of low reinforcement compared with high reinforcement.
4- Improving the total serviceability of the examined beams by increment either the number of FRCM layers or the reinforcement ratio.
5- Using PBO- FRCM system is more significant compared with other types of FRCM layer.
6- The ductility decreases as the number of FRCM layers, or the reinforcement ratio are increased.
7- Usage U-wrapped FRCM layer is more significant compared with the straight FRCM layer.

References

[1] Toutanji, H., et al. (2006). Flexural behavior of reinforced concrete beams externally strengthened with CFRP sheets bonded with an inorganic matrix. Engineering structures, 28(4), 557-566.

[2] Akbarzadeh, H., & Maghsoudi, A. A. (2010). Experimental and analytical investigation of reinforced high strength concrete continuous beams strengthened with fiber reinforced polymer. Materials & Design, 31(3), 1130-1147.

[3] Hawileh, R. A., et al. (2014). Behavior of reinforced concrete beams strengthened with externally bonded hybrid fiber reinforced polymer systems. Materials & Design, 53, 972-982.

[4] Obaidat, Y. T., et al. (2011). Retrofitting of reinforced concrete beams using composite laminates. Construction and Building Materials, 25(2), 591-597.

[5] Ahmed, A., & Kodur, V. (2011). The experimental behavior of FRP-strengthened RC beams subjected to design fire exposure. Engineering Structures, 33(7), 2201-2211.

[6] Ahmed, A., & Kodur, V. K. R. (2011). Effect of bond degradation on fire resistance of FRP-strengthened reinforced concrete beams. Composites Part B: Engineering, 42(2), 226-237.

[7] Silva, M. A., & Biscaia, H. (2008). Degradation of bond between FRP and RC beams. Composite structures, 85(2), 164-174.

[8] Hashemi, S., & Al-Mahaidi, R. (2012). Flexural performance of CFRP textile-retrofitted RC beams using cement-based adhesives at high temperature. Construction and Building Materials, 28(1), 791-797.

[9] Hawileh, R. A., et al. (2015). Temperature effect on the mechanical properties of carbon, glass and carbon–glass FRP laminates. Construction and Building Materials, 75, 342-348.

[10] Ombres, L. (2011). Flexural analysis of reinforced concrete beams strengthened with a cement based high strength composite material. Composite Structures, 94(1), 143-155.

[11] Jabr, A., et al. (2017). Effect of the fiber type and axial stiffness of FRCM on the flexural strengthening of RC beams. Fibers, 5(1).

[12] Elghazy, M., et al. (2017). Effect of corrosion damage on the flexural performance of RC beams strengthened with FRCM composites. Composite Structures, (180), 994-1006.

[13] Aljazaeri, Z. R., et al. (2019). A novel and effective anchorage system for enhancing the flexural capacity of RC beams strengthened with FRCM composites. Composite Structures, 210, 20-28.

[14] Donnini, J., et al. (2017). Fabric-reinforced cementitious matrix behavior at high-temperature: Experimental and numerical results. Composites Part B: Engineering, 108, 108-121.

[15] Abaqus. Version 6.14. Dassault Systemes: 3DS Paris Campus; 2014.

[16] Michał, S., & Andrzej, W. (2015). Calibration of the CDP model parameters in Abaqus. The 2015 Wourld Congress on Advances in Structural Engineering and Mechanics (ASEM15)

[17] Carreira, D. J., & Chu, K. H. (1985). Stress-strain relationship for plain concrete in compression. Journal Proceedings (Vol. 82, No. 6, pp. 797-804)

[18] Salve, A. K., & Jalwadi, S. N. (2015). Implementation of cohesive zone in ABAQUS to investigate fracture problems. Proceedings of the National Conference for Engineering Post Graduates RIT, NConPG–15, (pp. 60-66)

[19] Ombres, L. (2012). Debonding analysis of reinforced concrete beams strengthened with fibre reinforced cementitious mortar. Engineering Fracture Mechanics, 81, 94-109.

[20] Ombres, L. (2015). Analysis of the bond between fabric reinforced cementitious mortar (FRCM) strengthening systems and concrete. Composites Part B: Engineering, 69, 418-426.

[21] Younis, A., & Ebead, U. (2018). Bond characteristics of different FRCM systems. Construction and Building Materials, 175, 610-620.

[22] Grande, E., et al. (2018). Numerical investigation on the bond behavior of FRCM strengthening systems. Composites Part B: Engineering, 145, 240-251.

[23] Grande, E., et al. (2019). Numerical simulation of the de-bonding phenomenon of FRCM strengthening systems. Frattura ed Integrità Strutturale, 13(47), 321-333.

[24] Nagah, M., et al. (2020). Nonlinear Finite-Element Analysis for RC Beams Strengthened with Fabric-Reinforced Cementitious Matrix. JES. Journal of Engineering Sciences, 48(4), 554-576.